

# Probing the electron–LO-phonon interaction of a single impurity state in a semiconductor

U. Woggon and E. Lüthgens

*Fachbereich Physik, Universität Dortmund, Otto-Hahn-Strasse 4, D-44227 Dortmund, Germany*

H. Wenisch and D. Hommel

*Institut für Festkörperphysik, Universität Bremen, Kufsteiner Strasse 1, D-28359 Bremen, Germany*

(Received 2 November 2000; published 31 January 2001)

The photoluminescence of single emission centers in the energy range of donor-acceptor pair transitions is studied in ZnSe by spatially resolved imaging spectroscopy at the diffraction limit. Addressing single impurity states, the electron–LO-phonon interaction is probed locally and a microscopic Huang-Rhys parameter between  $S=0.08$  and  $0.51$  is found, related to a variation of the homogeneous linewidth between  $1$  meV and  $15$  meV. Based on our results the donor-acceptor pair model is reconsidered in the limit of large variation of the pair energies  $\Delta(E_A+E_D) > \hbar\omega_{LO}$ .

DOI: 10.1103/PhysRevB.63.073205

PACS number(s): 71.55.Gs, 78.55.Et

Optical addressing of single, light-emitting states is a challenge for high-resolution spectroscopy. In semiconductors, emission from single, quasi zero-dimensional excitons is studied, e.g., in nanocrystals or self-assembled, epitaxially grown islands,<sup>1–6</sup> whereas less attention is paid to impurities. Spectroscopy of single impurities, however, would open the way to study such fundamental phenomena as coherence time, LO-phonon coupling strength, or changes of energy states in external fields for an individual, discrete-level system in a semiconductor. An interesting example is the donor-acceptor pair (DAP) band, an intrinsically inhomogeneously broadened system that is presently only described with respect to its ensemble properties. Since the energy of the optical transition and the polarity of the wave function overlap depend on the different next-neighbor distances between donors and acceptors as well as on the different types of impurities involved, the spectrum of the individual pair transitions should be distinctly different from the ensemble average. In particular, the Huang-Rhys parameter  $S$  as a measure for the electron–LO-phonon coupling strength becomes a microscopic parameter and reflects the corresponding electron-hole distances. A way to adjust the wave function overlap of electrons and holes, if possible, could have implications for optimizing and controlling optical transition linewidths, i.e., coherence times.

In this Brief Report we report on the observation of a spatially varying electron–LO-phonon coupling strength found for impurities in the energy range of the donor-acceptor pair transitions in ZnSe. We will show that the various impurity states can be spectroscopically distinguished not only by their energies but also by a microscopic Huang-Rhys parameter  $S$ . The smallest observed values of  $S \sim 0.08$  suggest that coupling to the lattice environment can become small and decoherence can be suppressed for selected impurity states. Additionally, we found impurity states of the same energy but with different  $S$  as well as impurity states separated by just the energy of one LO phonon. Although these impurity states are all in the DAP energy range, the standard DAP model cannot be used to explain the photoluminescence (PL) spectrum of all defects observed.

The sample under study is a nominally undoped ZnSe layer ( $d=1$   $\mu\text{m}$ ) homoepitaxially grown on a ZnSe substrate.<sup>7</sup> For an overview, we discuss first in Fig. 1 the spatially integrated, i.e., macroscopic, photoluminescence. The spectrum is dominated by a strong signal due to the emission of free (FE's) and weakly bound excitons (BE's) at  $\sim 2.8$  eV and by a strong luminescence band at  $2.6$  eV ( $Y$  line) which is ascribed to radiative recombination of excitons localized at extended structural defects such as dislocations.<sup>8–11</sup> Around  $E=2.706$  eV we observe a weak emission at the energy expected for a donor-acceptor pair band and its LO-phonon replica ( $\hbar\omega_{LO}=31$  meV). The corresponding donor and acceptor energies are  $E_D=26$  meV and  $E_A \approx 80$ – $100$  meV (for a review of DAP energies, see Refs. 8,9,11–16).

Here we consider the donor-acceptor pair system as a model for a varying overlap of the electron and hole wave functions. The  $R$  dependence of the Huang-Rhys parameter  $S(R)$  can be calculated by a quantum defect model developed in Ref. 17. It has been recently applied to DAP's in ZnSe in Ref. 18 and is illustrated in the inset of Fig. 1. In this model, the envelope  $F_{e,h}(\mathbf{r})$  of the electron (hole) ground state bound to an impurity is given by

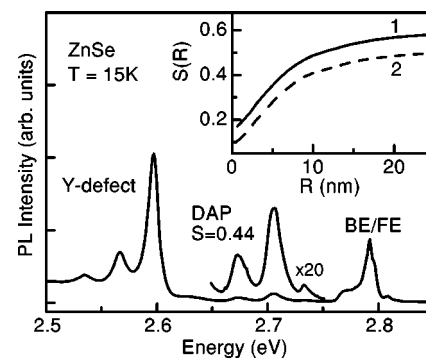


FIG. 1. PL spectra of a  $1$   $\mu\text{m}$  ZnSe epilayer for nonresonant excitation at  $3.5$  eV by a HeCd laser. The inset shows the theoretical  $S(R)$  dependence after Ref. 18 for  $E_D=30$  meV and  $E_A=80$  meV (1) and  $65$  meV (2).

$$F_{e,h}(\mathbf{r}) = N_{e,h,\nu} r^{\nu-1} \exp(-\mathbf{r}/\nu a^*), \quad (1)$$

where  $a^*$  is the effective Bohr radius of the defect state,  $N_{e,h,\nu}$  a normalization factor, and  $\nu$  the quantum defect parameter with  $\nu^2 = E_i^R/E_{A,D}$ .  $E_{A,D}$  are the experimentally observed ionization energies of donor and acceptor and  $E_i^R$  is the ionization energy of the hydrogenlike impurity.  $S(R)$  can be calculated according to

$$S(R) = \frac{e^2}{\pi \hbar \omega_{LO}} \left( \frac{1}{\epsilon_\infty} - \frac{1}{\epsilon_s} \right) \left[ \int_0^\infty [|\rho_e(q)|^2 + |\rho_h(q)|^2] dq - \int_0^\infty \rho_e(q) \rho_h(q) \frac{\sin(qR)}{qR} dq \right], \quad (2)$$

where  $\epsilon_\infty$  and  $\epsilon_s$  are the high-frequency and static dielectric constants.<sup>17–19</sup>  $\rho_{e,h}(q)$  is the Fourier transform of the charge density calculated with the wave functions  $F_{e,h}(\mathbf{r})$  from Eq. (1). In the inset of Fig. 1, the theoretical curve of  $S(R)$  is plotted for two examples: a hydrogenlike donor of  $E_D = 30$  meV and a nonhydrogenlike, shallow acceptor having an energy between  $E_A = 80$  meV and 65 meV, i.e., similar to the energy range of the observed impurity transitions. The theoretical estimate shows that a variation in the pair distance between 2 and 20 nm would result in a change of the microscopic  $S$  between  $\sim 0.1$  and  $\sim 0.5$ . The experimental value of  $S$  can be obtained from the intensity  $I$  of the zero-phonon line and the  $j$ th LO-phonon sidebands and obeys the equation  $I_j = (S^j/j!) \exp(-S)$ .<sup>15</sup> Fitting the line shape of the spatially integrated PL spectrum of Fig. 1, we obtain an averaged, i.e., macroscopic, value of  $S = 0.44$  which would correspond to an average DAP distance around  $R = 10$  nm in the framework of the standard donor-acceptor pair model.

In order to implement the variation of  $S$ , we have to solve the experimental problem of optically detecting the emission centers individually or, at least, to average over a much smaller number of impurity states in comparison with the macroscopic PL spectrum. The method used here is photoluminescence imaging at the diffraction limit for a sample with very low impurity concentration. The exciting light of a HeCd laser is focused into a  $100 \mu\text{m}$  spot on the sample. By means of a microscope objective with high numerical aperture (0.4), the light emitted by the sample, which is held in a microscope cryostat, is spectrally resolved by a 0.46 m spectrometer and imaged on the nitrogen-cooled, two-dimensional (2D) array of a charged-coupled device (CCD). Since the imaging spectrometer provides a correction of spherical and chromatic aberrations along both the lateral and vertical beam profiles, the whole area of the detector ( $1024 \times 256$  channels) can be used. The experimental setup provides a spatial dispersion of  $0.5 \mu\text{m}/\text{pixel}$  and a spectral dispersion of  $0.15 \text{ nm}/\text{pixel}$ . The left part of Fig. 2 shows a PL image measured at  $T = 6$  K. Emitting species of high concentrations, such as free and weakly bound excitons at  $E = 2.8$  eV, cannot be spatially resolved and result in a homogeneously distributed signal intensity over the whole detection area of the CCD. The emission around  $E = 2.6$  eV is imaged as a spotty pattern because of the lower concentration of the  $Y$  defects. Each line is accompanied by its LO-

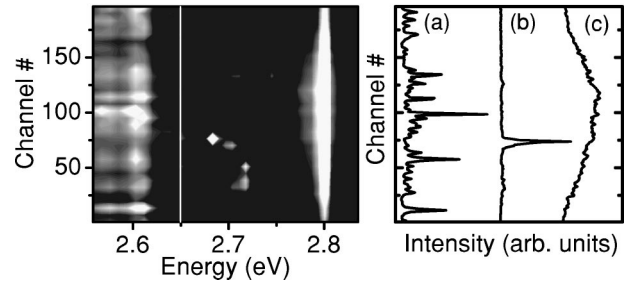


FIG. 2. Left: 2D photoluminescence image (logarithmic gray scale) detected by the  $1024 \times 256$  array of a cooled CCD camera. Above an energy  $E > 2.65$  eV (white line), the intensity is scaled by a factor of 10 to enhance the weak signal of single emission centers. Right: Signal per channel plotted for selected energies of (a) 2.606 eV, (b) 2.68 eV, and (c) 2.795 eV;  $T = 6$  K.

phonon replica. Between the energy of FE emission and of the  $Y$  defect, several bright, single spots appear in the energy range expected for the donor-acceptor pair transitions. In the right part of Fig. 2, the intensity distribution across the CCD is plotted for selected energy cuts. The minimum full width at half maximum (FWHM) measured for the sharpest peaks is 1.5 pixels. By reading out the spectra for each channel separately, we are thus able to measure the local PL signal from a  $750 \text{ nm}$  spot on the sample. As can be seen in Fig. 2, the very low impurity concentration allows us to detect spatially well-separated, single bright spots due to impurity emission. Within the energy range of the donor-acceptor pair transitions considered here, we expect additional recombination centers formed by impurity complexes, involving, e.g., vacancies or other structural defects. Since we are studying nominally undoped samples, the concentration of acceptors can be lower than the donor concentration, resulting in a spatial “dilution” of the DAP recombination centers.

The problem of varying the pair distance  $R$  we solve by controlling the average population of donors and acceptors, i.e., the average number of donors and acceptors available for a pair transition. A suitable parameter to influence the mean  $R$  of the ensemble is the temperature. A slight increase in temperature starting from 6 K via 11 K up to 20 K results in an increase of neutral donors and acceptors, e.g., due to an increase in the diffusion lengths of free electrons and holes, or due to the release of weakly bound excitons from donors or acceptors. For temperatures  $T > 60$  K, the increasing diffusion into the substrate with considerably higher impurity concentration results in an upper limit for our spatial resolution, and for even higher temperatures again in a measurement of an averaged Huang-Rhys parameter.

In Fig. 3 the change in the PL image is shown when the temperature is gradually increased (see also Fig. 2 for  $T = 6$  K). The CCD array (left part) shows the change in impurity concentration, which is equivalent to a variation of the average pair distance  $R$ . Whereas up to  $T = 11$  K the spotty pattern is still preserved and single emission centers can still be resolved, we observe for  $T = 60$  K an almost homogeneously illuminated CCD image around 2.7 eV (high density of DAP’s, only limited spatial resolution of single pairs). For both temperatures, a few exemplary spectra of selected CCD

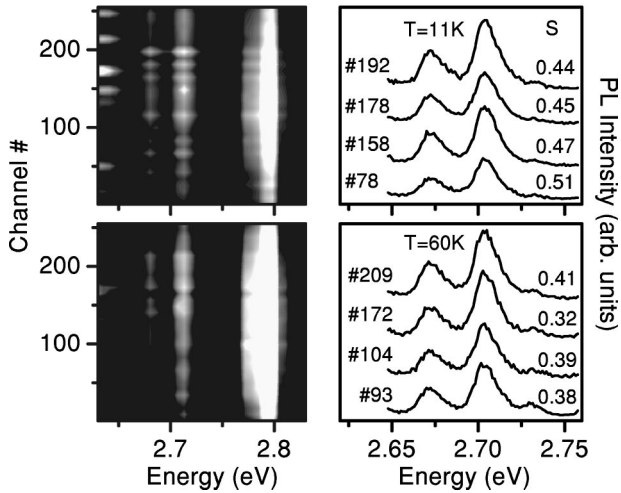


FIG. 3. Left: 2D PL image at  $T=11\text{ K}$  (upper) and  $60\text{ K}$  (lower) showing the decrease in spatial resolution with increasing temperature. Right: PL spectra of DAP transitions measured for selected CCD channels. The corresponding Huang-Rhys parameter  $S$  is given on the right.

channels (bright spots) are plotted on the right part of Fig. 3 together with the fitted Huang-Rhys parameter  $S$ . Comparing the results for  $T=60\text{ K}$  and  $T=11\text{ K}$ ,  $S$  has the clear tendency of becoming smaller for higher DAP concentrations (small values of  $R$ ) because of the increase of impurities available for a DAP transition at higher temperatures. Spectra measured at  $20\text{ K}$  and  $40\text{ K}$  (not shown here) also follow this trend. A further decrease in  $S$  for even higher temperatures  $T>80\text{ K}$  is limited because the PL spectrum is then dominated by the free-to-bound transition of the acceptor state, which is found at an energy of  $2.703\text{ eV}$ .

Figure 4 summarizes the observed variation in  $S$  in the temperature range  $T\geq 11\text{ K}$  for emission centers having their energy in the range of DAP transitions. In Fig. 4(a) examples are given for the highest and lowest values of  $S$  observed (the PL intensity has been normalized to the maximum of the

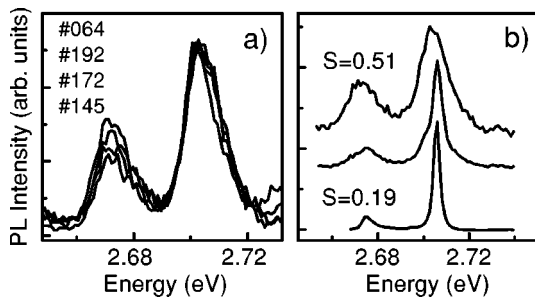


FIG. 4. (a) Normalized PL spectra at different channels and temperatures illustrating the observed variation of  $S$ . From top to bottom: channels 64 and 192 are measured at  $T=11\text{ K}$  with  $S=0.51$  and  $0.44$ , respectively, channels 172 and 145 are measured at  $T=60\text{ K}$  giving  $S=0.32$  and  $0.30$ . (b) PL spectra from different spots on the sample measured at highest spatial resolution and lowest temperature  $T<11\text{ K}$  showing the coexistence of two types of emission centers of the same energy but with high and low Huang-Rhys parameters  $S$ .

zero-phonon line). The determined Huang-Rhys parameter  $S$  changes from  $0.51$  at  $11\text{ K}$  (which corresponds from Fig. 1 to  $R$  between  $10\text{ nm}$  and  $20\text{ nm}$ ) to  $S=0.3$  at  $T=60\text{ K}$ . Here we observe the unusual behavior of a *decreasing electron-LO-phonon coupling with increasing temperature*, which is, however, in agreement with the DAP model discussed above. Because the low value of  $S$  corresponds to a small DAP distance of  $R$  around  $5\text{ nm}$  and therefore to a very high average DAP concentration, we indeed detect at  $T=60\text{ K}$  partly signals arising from the substrate with higher doping, in agreement with the observed loss in spatial resolution shown in Fig. 3.

In the final part of the paper we will address the behavior observed at the lowest temperatures  $T\leq 6\text{ K}$ . Assuming further the validity of the DAP model, we should find the highest values for the Huang-Rhys parameter  $S$  because of the lowest DAP concentration and thus largest values of  $R$  (see Fig. 1). The estimated average distance  $R$  is expected to become distinctly larger than the excitonic Bohr radius of the free exciton in ZnSe ( $a_B^{\text{ex}}=4.5\text{ nm}$ ). It will be shown in the following that our results at the lowest temperatures are in disagreement with the DAP model and an alternative explanation based on localized excitons will be proposed. As illustrated in Fig. 4(b), we observe for the lowest temperatures an unexpected feature, which we will discuss in the following in more detail.

At  $T=6\text{ K}$  a second type of emission center is observed with transition energies in the same spectral range as the DAP energies but with a very different electron-LO-phonon coupling strength. As shown in Fig. 4(b), this peak is sometimes visible as a superposition of a broad and narrow peak structure at  $T=11\text{ K}$  and dominates the emission at certain sample spots at the lowest temperatures of  $T=6\text{ K}$ . Significant for the second type of emission center a very small linewidth and a very low  $S\sim 0.2$ , in contrast to the expected value of  $S\geq 0.5$  according to the DAP model. These single, bright spots can clearly be spatially resolved and the spectra can be measured very accurately for the single emission centers. A statistical analysis of energies and Huang-Rhys parameters was performed for about 40 individual impurity states all emitting at  $T=6\text{ K}$  in the energy range of the DAP transition (Fig. 5). Whereas the inhomogeneously broadened, spatially integrated spectrum shows a typical DAP band with a FWHM of  $14.8\text{ meV}$  and a Huang-Rhys factor of  $S\approx 0.4$ , the homogeneous linewidth of a single peak is only  $1$  to  $4\text{ meV}$ , as the spectra (b) and (c) demonstrate in Fig. 5, and the microscopic  $S$  is in disagreement with the predictions of the DAP model. An accumulation of peaks around  $2.68\text{ eV}$  is found, which by chance coincide with the energy of the LO-phonon replica of the  $2.71\text{ eV}$  emission. Thus the spectral analysis and statistics of single transitions reveal that in the spatially integrated spectra studied until now *a much stronger intensity of the LO-phonon replica was inferred due to the superposition of low-energy peaks and LO-phonon replicas of high-energy peaks*. This result demonstrates that in the limit of large variation in the pair energies  $\Delta(E_A+E_D) > \hbar\omega_{\text{LO}}$  the traditional DAP model cannot be used to fit the ensemble PL.

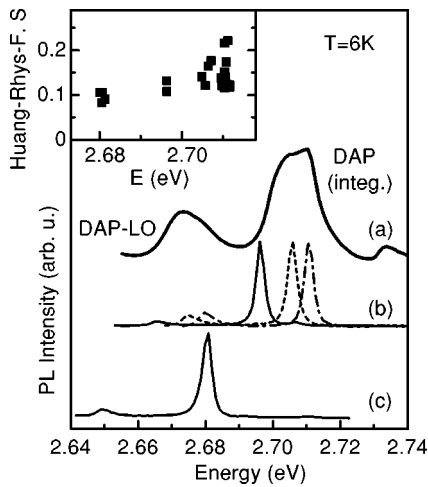


FIG. 5. (a) Spatially integrated, averaged PL band in the energy range of DAP transitions and its LO-phonon replica (macroscopic  $S \approx 0.4$ ) and representative, normalized single-channel spectra for different energies (b) and (c). The inset shows the statistics obtained for the microscopic  $S$  at  $T = 6$  K.

The very small values of  $S$  between 0.08 and 0.23 (see inset of Fig. 5) measured at the lowest temperatures and indicating a weak coupling to LO phonons can be explained in two ways: (i) only the pairs closest in distance  $R$  contribute to the emission and we observe three types of DAP involving different acceptors with transition energies centered around 2.680 eV, 2.697 eV, and 2.708 eV, or (ii) we no longer observe DAP transitions but *excitons* bound to single, deep defect potentials. Since the hypothesis (i) would correspond to values of  $R < 2$  nm, which is considerably smaller

than  $a_B^{\text{ex}}$  in ZnSe and would imply a huge impurity concentration where the individual emission sites are no longer spatially resolvable, in contrast to our experiment, we prefer (ii) to explain the observed small values of  $S$ . This assumption is supported by experimental data reported for excitons localized, e.g., in single, nanometer-sized epitaxially grown CdSe islands.<sup>5</sup> There, the Huang-Rhys parameter for a three-dimensionally confined exciton is determined as  $S = 0.04$  and explained by a decrease in polarity of the excitonic wave function because of quantum confinement. Generalizing, when a local potential exists that is strong enough to localize electrons *and* holes within a volume below the bulk excitonic Bohr radius  $a_B^{\text{ex}}$ , the Huang-Rhys parameter becomes small.

Summarizing, experimental evidence for a spatially varying electron-LO-phonon coupling has been obtained. The variation of the microscopic  $S$  indicates that the homogeneous linewidth is not an unchangeable parameter but can be manipulated whenever an engineering of the polarity of the electron-hole pair wave function succeeds. Considering the large differences in the published data for homogeneous linewidths in the case of localized electron-hole pairs in semiconductor nanostructures, an optimization of the sample growth and structure that excludes any trapping of electrons or holes separately, or internal electric fields or large differences in dielectric constants might result in such an engineering of the wave function overlap and thus in optimizing of coherence times.

Financial support by the Volkswagen Foundation within the Photonics Program and by the Ministerium für Bildung und Wissenschaft des Landes Nordrhein-Westfalen is gratefully acknowledged.

- <sup>1</sup>J.-Y. Marzin, J.M. Gerard, A. Izrael, D. Barrier, and G. Bastard, Phys. Rev. Lett. **73**, 716 (1994).
- <sup>2</sup>D. Gammon, E.S. Snow, B.V. Shanabrook, D.S. Katzer, and D. Park, Phys. Rev. Lett. **76**, 3005 (1996).
- <sup>3</sup>S.A. Empedocles, D.J. Norris, and M.G. Bawendi, Phys. Rev. Lett. **77**, 3873 (1996).
- <sup>4</sup>V.D. Kulakovskii, G. Bacher, R. Weigand, T. Kümmell, A. Forchel, E. Borovitskaya, K. Leonardi, and D. Hommel, Phys. Rev. Lett. **82**, 1780 (1999).
- <sup>5</sup>F. Gindele, K. Hild, W. Langbein, and U. Woggon, Phys. Rev. B **60**, R2157 (1999).
- <sup>6</sup>F. Koberling, A. Mews, and Th. Basche, Phys. Rev. B **60**, 1921 (1999).
- <sup>7</sup>H. Wenisch, M. Fehrer, K. Ohkawa, D. Hommel, M. Prokesch, U. Rinas, and H. Hartmann, J. Appl. Phys. **82**, 4690 (1997).
- <sup>8</sup>H. Gumlich, A. Theis, and D. Tschierse, in *Numerical Data Functional Relationships in Science and Technology*, edited by O. Madelung, Landolt-Börnstein, New Series, Group III, Vol. 17, pt. 6 (Springer, Berlin, 1982), pp. 132–135.
- <sup>9</sup>J. Gutowski, N. Presser, and G. Kudlek, Phys. Status Solidi A

- 120**, 11 (1990).
- <sup>10</sup>K. Shahzad, J. Petruzzello, D.J. Olega, D.A. Cammack, and J.M. Gaines, Appl. Phys. Lett. **57**, 2452 (1990).
- <sup>11</sup>P.J. Dean, Phys. Status Solidi A **81**, 625 (1984).
- <sup>12</sup>P. Bäume, S. Strauf, J. Gutowski, M. Behringer, and D. Hommel, J. Cryst. Growth **184/185**, 531 (1998); P. Bäume, M. Behringer, J. Gutowski, and D. Hommel, Phys. Rev. B **62**, 8023 (2000).
- <sup>13</sup>P. Bäume, J. Gutowski, D. Wiesmann, R. Heitz, A. Hoffmann, E. Kurtz, D. Hommel, and G. Landwehr, Appl. Phys. Lett. **67**, 1914 (1995).
- <sup>14</sup>D.G. Thomas, M. Gershenson, and F.A. Trumbore, Phys. Rev. **133**, A269 (1964).
- <sup>15</sup>O. Goede and E. Gutsche, Phys. Status Solidi **17**, 911 (1966).
- <sup>16</sup>P.J. Dean and R.L. Merz, Phys. Rev. **178**, 1310 (1969).
- <sup>17</sup>H.B. Bebb, Phys. Rev. **185**, 1116 (1969).
- <sup>18</sup>A.L. Gurskii and S.V. Voitkov, Solid State Commun. **112**, 339 (1999).
- <sup>19</sup>M. Soltani, M. Certier, R. Evrard, and E. Kartheuser, J. Appl. Phys. **78**, 5626 (1995).